Spontaneous Pattern Formation in an Antiferromagnetic Quantum Gas

Jochen Kronjäger,[1,2] Christoph Becker,[2] Parvis Soltan-Panahi,[2] Kai Bongs,[1,2] and Klaus Sengstock[2]

[1]*MUARC, School of Physics and Astronomy, University of Birmingham, Edgbaston, Birmingham B15 2TT, United Kingdom*

[2]*Institut für Laser-Physik, Universität Hamburg, Luruper Chaussee 149, 22761 Hamburg, Germany*

(Received 9 July 2010; published 24 August 2010)

In this Letter we report on the spontaneous formation of surprisingly regular periodic magnetic patterns in an antiferromagnetic Bose-Einstein condensate (BEC). The structures evolve within a quasi-one-dimensional BEC of ^{87}Rb atoms on length scales of a millimeter with typical periodicities of $20 \ldots 30$ μm, given by the spin healing length. We observe two sets of characteristic patterns which can be controlled by an external magnetic field. We identify these patterns as linearly unstable modes within a mean-field approach and calculate their mode structure as well as time and energy scales, which we find to be in good agreement with observations. These investigations open new prospects for controlled studies of symmetry breaking and complex quantum magnetism in bulk BEC.

DOI: 10.1103/PhysRevLett.105.090402 PACS numbers: 05.30.Jp, 03.75.Mn, 32.60.+i, 67.85.−d

Spontaneous pattern formation is a phenomenon ubiquitous in nature. In particular it is a common theme between two fields of physics — phase transitions and nonlinear dynamic systems. Phase transitions are often associated with an equilibrium or ground state that breaks the translational symmetry of the underlying system, observable as spatial structure. In extended nonlinear systems, on the other hand, structure may emerge as unstable modes grow exponentially, amplifying a small initial fluctuation. Bose-Einstein condensates of alkali atoms offer unique opportunities to study both nonlinear dynamics [1–5] and phase transitions [6–8] in the quantum regime. Spinor Bose-Einstein condensates are of particular interest due to their links with magnetic condensed matter systems.

Recent theoretical work on spatial structure formation in spinor condensates has largely focused on the ferromagnetic phase of $F = 1$ ^{87}Rb Bose-Einstein condensates [9–16], following the first ground-breaking experiments [17,18]. In this system, structure formation is intuitively understood as spatial separation of different spin states into ferromagnetic domains. In addition, the dipole-dipole interaction was found to play an important role in this system [19–21]. In contrast, pattern formation in antiferromagnetic systems is less intuitive and to our knowledge has only been addressed in one very recent experiment [22]. There it was found that the trapping potential plays an important role in inducing pattern-forming resonances.

In this Letter we report the first observation of spontaneous formation of regular spin structures in a quasi-1D antiferromagnetic spinor condensate. In particular, we discuss the emergence of different spin-wave patterns as a function of the external magnetic field and we show that these patterns can be associated with unstable modes of the Gross-Pitaevskii equation.

In our experiment, we prepare ^{87}Rb $F = 2$ atoms in the fully stretched state in a transverse direction, such that the spin vector is $\langle \vec{F} \rangle = 2\vec{e}_x$ in the corotating frame [23] [see Fig. 2(a)]. This state maximizes the mean-field energy and is therefore stationary but energetically unstable at zero magnetic field, analogous to an inverted pendulum. Adding a spatial degree of freedom thus makes it an ideal starting point to investigate the formation of excited state patterns. These patterns remain relatively stable due to the excellent thermal insulation of cold atom systems. This approach follows the concept of nonlinear dynamic evolution.

In order to study spatial pattern formation in the simplest nontrivial case, we have developed a reliable method to create extremely elongated Bose-Einstein condensates in the optical potential of a single focused laser beam, with trap frequencies $\omega_{x,y,z} = 2\pi \times (85, 133, 0.8)$ Hz. The condensates are approximately 800 μm long and the calculated Thomas-Fermi radii perpendicular to the long axis are 2.9 μm horizontally and 4.5 μm vertically. In the transverse direction, the spin healing length $\xi_s = \sqrt{\hbar^2/2mg_1\langle n \rangle} \approx 3.4$ μm is on the order of the size of the condensate, effectively suppressing transverse spin structure and creating a quasi-1D geometry. A variable and approximately homogeneous magnetic field, whose axial gradient is canceled with a remaining curvature of 60 mG cm^{-2}, is aligned with the axis of the trap. Transverse residual magnetic fields are compensated to less than 0.5 mG. The transverse stretched state is prepared from the $|F = 1, m_F = -1\rangle$ state by first adiabatically transferring the atoms to $|F = 2, m_F = -2\rangle$ using a microwave sweep and subsequently rotating the stretched state into the transverse direction using a $\pi/2$ radio frequency pulse. Finally, Stern-Gerlach separation during a short time of flight allows us to image the individual spin densities with a spatial resolution of ~ 2 μm.

As a central result Fig. 1 shows the markedly regular wavelike spin patterns that emerge after several hundred milliseconds of free evolution in the elongated trap. These patterns reveal two regimes with distinct symmetries, which depend on the external magnetic field. At low mag-

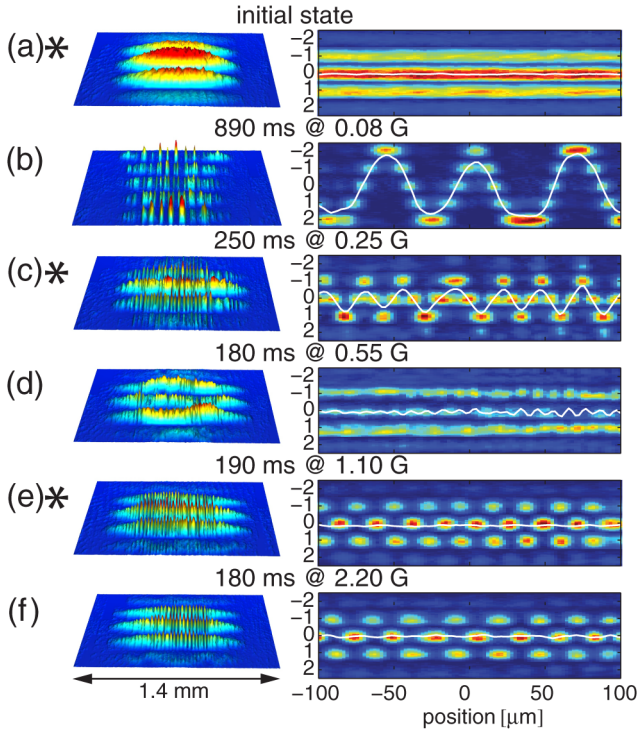

FIG. 1 (color online). Initial state (a) and saturated spin patterns arising in spinor condensates for increasing magnetic field (b)–(f). The individual 3D rendered false color absorption profiles in each image visualize the spatial density distribution for each of the five magnetic projections $m_F = -2 \ldots + 2$ of the $F = 2$ hyperfine manifold. Imperfections in the preparation and detection artifacts (e.g., optical interference fringes), which appear as fluctuations visible in the initial state (a), are distinctly different from the patterns of (b)–(f). The cases marked "*" are chosen to represent the initial state, the interaction dominated regime, and the Zeeman-dominated regime, respectively, and are referred to in the following figures.

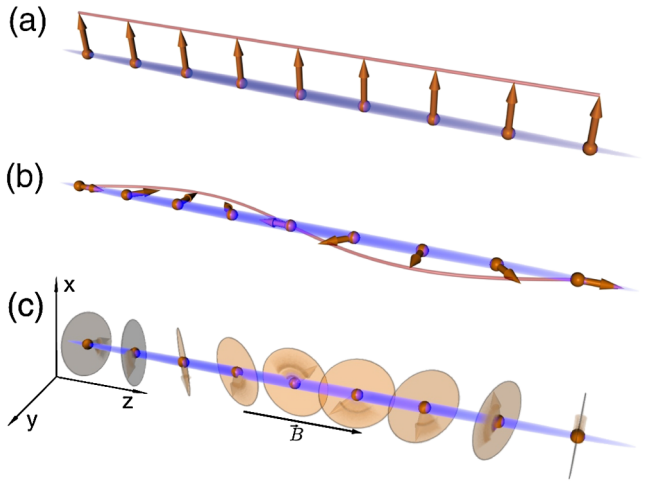

FIG. 2 (color online). Simplified illustration of the local spin vector in Figs. 1(a), 1(c), and 1(e) (marked "*"). (a) Initial state, the spin vector is fully stretched and points in the transverse x direction. (b) Interaction dominated regime, the spin vector is fully stretched but rotates from axial to transverse and back over one spatial period. (c) Zeeman-dominated regime, the local spin vector has zero length but still a defined orientation ($m_F = 0$ state) that rotates from axial to transverse and back.

netic field [Figs. 1(b) and 1(c)] the pattern is antisymmetric with respect to positive and negative m_F, indicating an alternating nonzero axial magnetization. It thus not only breaks translational symmetry but also the $m_F \rightarrow -m_F$ symmetry of the initial spin state. The data suggest that in this regime both the periodicity and growth rate scale with the magnetic field [24]. In contrast, at high magnetic field [Figs. 1(e) and 1(f)] the characteristic pattern is symmetric with respect to m_F and the axial component of the spin vector F_z remains zero everywhere. In this regime periodicity and growth rate do not change significantly with the magnetic field. The crossover regime at intermediate field [Fig. 1(d)] shows a less pronounced and irregular spin structure. In all cases the patterns are transient and slowly decay into a chaotic small-scale structure after several hundred milliseconds.

Figure 2 shows a simplified illustration of the patterns in terms of local spin orientation. At low magnetic field [Fig. 2(b)], the fully developed pattern appears as a stretched state rotating in the yz plane as a function of the z coordinate. This results in alternating "domains" of oppositely oriented axial magnetization, separated by transversely magnetized "domain walls." At high magnetic field [Fig. 2(c)], the pattern resembles an $m_F = 0$ state whose axis of quantization oscillates from axial to transverse and back.

The dynamics of spinor BEC is well captured by the time-dependent Gross-Pitaeskii equation, which for the case of constant density n can be written in terms of the local spinor $\zeta_{m=-F\ldots F}$ as $(\mu + i\hbar\partial/\partial t)\zeta_m = \partial\mathcal{H}/\partial\zeta_m^*$. The energy functional $\mathcal{H}$ comprises kinetic energy, quadratic Zeeman effect, and interaction energy (given here for $F = 2$),

$$\mathcal{H} = \mathcal{H}_{\mathrm{kin}} + q\langle F_z^2\rangle + \frac{n}{2}[g_0 + g_1\langle\vec{F}\rangle^2 + g_2|S_0|^2], \quad (1)$$

where $\langle\cdot\rangle$ denotes the local expectation value of the respective spin operator and $S_0 = \zeta_{+2}\zeta_{-2} - \zeta_{+1}\zeta_{-1} + \zeta_0^2/2$ is the local spin-singlet amplitude [25–27]. The interaction parameters $g_{0,1,2}$ are determined from the s-wave scattering lengths and correspond to the spin-independent (g_0) and spin-dependent ($g_{1,2}$) parts of the mean-field interaction, respectively. In our case, the g_2 contribution is negligible and will be dropped in the following for the sake of clarity. It is, however, included in our numerical calculations in the low-field case.

Previous experiments [23] have shown that spin dynamics in the single-mode limit is driven purely by the competition of quadratic Zeeman energy $q\langle F_z^2\rangle$ and spin-dependent interaction energy $g_1 n\langle\vec{F}\rangle^2/2$, defining two limiting cases — the interaction dominated regime at low

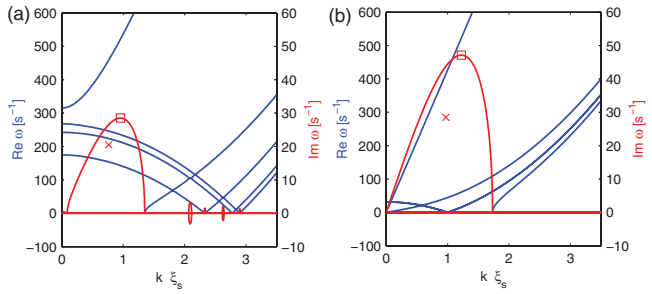

FIG. 3 (color online). Bogoliubov spectra resulting from a linear stability analysis of the 1D GPE, (a) Interaction regime at 0.25 G, (b) Zeeman regime at ∞G. The interaction parameter $g_1\langle n\rangle = 2\pi \times 5$ Hz is obtained from the observation of homogeneous spin oscillations. For $F = 2$, five pairs of complex conjugate branches exist (of which only the positive real frequencies are plotted). Branches with positive imaginary frequency indicate unstable modes. Compare the most unstable modes (squares) to the observed modes (crosses).

magnetic field ($g_1 n \gg q$) and the Zeeman-dominated regime ($g_1 n \ll q$) at high field. The two regimes are separated by a crossover resonance where spin oscillation amplitudes are dramatically enhanced while time scales diverge. In the following, $B = 0.25$ G ($g_1 n/q = 1.1$) and $B = 1.1$ G ($g_1 n/q = 0.06$) will be used as representatives of the interaction and Zeeman regime, respectively [28].

In order to identify the unstable modes corresponding to the observed patterns in the interaction and Zeeman regime, we perform a linear stability analysis of the Gross-Pitaevskii equation around a stationary state close to the initial state prepared in the experiment. In the interaction regime, i.e., for low magnetic fields, we analytically linearize the GPE using a Bogoliubov ansatz. The stationary state close to the initial state is obtained numerically from the full GPE, and the corresponding Bogoliubov matrices are numerically diagonalized to obtain the spectrum and modes (Fig. 3).

In the Zeeman regime, i.e., for high magnetic field, the quadratic Zeeman effect induces oscillations of the spin on a much shorter time scale than pattern formation. We eliminate this fast dynamics by applying a unitary transformation $U = \exp(-iqF_z^2 t/\hbar)$ and then dropping all explicitly time dependent terms from the linearized equations (rotating wave approximation, RWA). Physically, this amounts to averaging interactions over the spin oscillations induced by the quadratic Zeeman effect. The RWA fully removes the magnetic field dependence and allows us to analytically find a stationary state $|\zeta_0\rangle = (0, 1/2, \sqrt{1/2}, 1/2, 0)$, which again is close to the actual initial state. We then proceed as in the low-field case to obtain the spectrum (Fig. 3).

In both the interaction- and Zeeman-dominated regime a single unstable mode exists, indicated by an imaginary frequency over a certain range of wave vectors. Modes with a complex frequency exponentially grow in time and lead to spontaneously formed patterns by amplification of arbitrarily small seeds. The characteristic spin pattern of the identified modes indeed coincides very well with the patterns observed experimentally (Fig. 4), suggesting s-wave interactions as the dominant mechanism in their formation. The linear instability predicted by the above analysis is further confirmed by the exponential growth of the modes as obtained from cross correlations of the measured spin densities (Fig. 5).

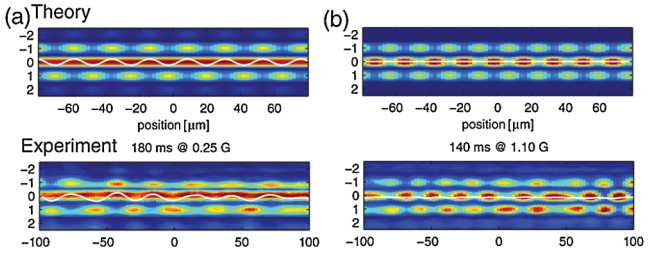

FIG. 4 (color online). Comparison of simulated Stern-Gerlach images with experimental data in the linear growth regime, (a) interaction dominated regime 0.25 G, (b) Zeeman-dominated regime ∞G. The mode pattern of the calculated most unstable modes coincide with the experimentally observed modes during linear growth.

A quantitative comparison of the experimental data to Bogoliubov theory (Fig. 3) reveals that at both $B = 0.25$ G and $B = 1.1$ G, the wavelength is approximately 20%

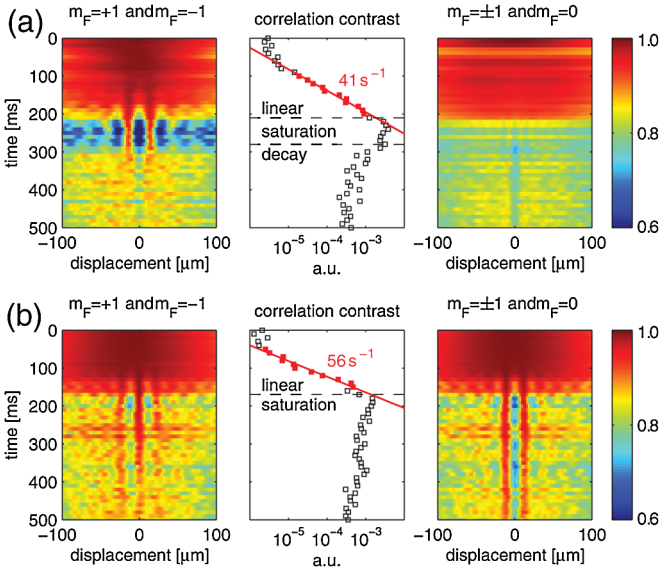

FIG. 5 (color online). Cross correlations of spin densities. (a) Interaction regime at 0.25 G, (b) Zeeman regime at 1.1 G. Color-coded plots (left and right) of the normalized correlation as a function of relative axial displacement and time of evolution allow to determine the symmetry and spatial periodicity of the evolving modes—(a) 28 μm and (b) 22 μm. The correlation contrast (center) can be tracked over 2 orders of magnitude and allows us to extract the growth rate of the mode (half the growth rate of the correlation function)—(a) 20 s^{-1} and (b) 28 s^{-1}.

larger than predicted. Note that in both regimes it is on the order of $2\pi\times$ the spin healing length $\xi_s = 3.4$ μm and much larger than the transverse size of the condensate, justifying *a posteriori* our assumption of a quasi-1D geometry. The growth rate of the mode amplitude is 30%–40% less than predicted. This is in reasonable agreement with our mean-field calculations, taking into account the approximations made in neglecting the axial trapping potential and the limitations of a linearized Bogoliubov approach. With the very good agreement in the mode structure and the clearly exponential growth observed, we are confident to have correctly identified the mechanism of pattern formation.

In conclusion, we have reported the spontaneous formation of regular spin patterns in an antiferromagnetic Bose-Einstein condensate. Pattern formation occurs in one of two distinct modes of characteristic symmetry, controlled by the relative size of interaction and quadratic Zeeman energy. We have been able to identify specific linear instabilities of a simplified mean-field model as the driving force of this breaking of translational symmetry. Our results thus demonstrate that purely local antiferromagnetic interactions suffice to generate ordered spin textures, in contrast to recent observations in ferromagnetic ^{87}Rb $F = 1$ [18]. Our experiment and analysis also provide a visual illustration of spatial multimode decoherence processes as anticipated in [23], also linking it to decoherence studies based on the Luttinger approach [29,30].

While linear stability analysis provides a conclusive explanation of the variety and dynamics of modes observed in experiment, it is a purely classical approach in character. However, our work also opens a new perspective towards fundamental quantum mechanical aspects of ultracold matter. For example, having observed exponential growth, the question of the origin of the fluctuations triggering this growth immediately arises [31,32]. A back-of-the-envelope calculation [33] provides an estimated initial modulation on the order of the shot-noise of the number of atoms contained within one half wavelength for our experiment, suggesting that quantum effects might play a significant role. Another interesting issue arises from the similarities between coherent dynamics in spinor BEC and optical nonlinearities. Interpreting density patterns as interference between left- and right-propagating modes suggests the possibility of entanglement as in spontaneous parametric down-conversion. Thus, spinor Bose-Einstein condensates may turn out to provide a new versatile tool to explore quantum effects in nonlinear dynamics.

We thank M. Baumert (University of Birmingham) for the 3D artwork in Figs. 1 and 2 as well as help with graphic design in general. We thank the Deutsche Forschungsgemeinschaft for support within the Forschergruppe FOR801. P. S. acknowledges support through DFG GRK 1355. K. B. thanks the EPSRC for financial support through Grant No. EP/E036473/1.

A very recent work by M. Matuszewski [34] discusses similar spin structures for $F = 1$ condensates in the context of roton instabilities.

[1] L. Deng *et al.*, Nature (London) **398**, 218 (1999).
[2] G. K. Campbell *et al.*, Phys. Rev. Lett. **96**, 020406 (2006).
[3] J. Denschlag *et al.*, Science **287**, 97 (2000).
[4] S. Burger *et al.*, Phys. Rev. Lett. **83**, 5198 (1999).
[5] C. Becker *et al.*, Nature Phys. **4**, 496 (2008).
[6] M. Greiner *et al.*, Nature (London) **415**, 39 (2002).
[7] Z. Hadzibabic *et al.*, Nature (London) **441**, 1118 (2006).
[8] K. Baumann *et al.*, Nature (London) **464**, 1301 (2010).
[9] W. Zhang *et al.*, Phys. Rev. Lett. **95**, 180403 (2005).
[10] H. Saito and M. Ueda, Phys. Rev. A **72**, 023610 (2005).
[11] M. Uhlmann, R. Schützhold, and U. R. Fischer, Phys. Rev. Lett. **99**, 120407 (2007).
[12] B. Damski and W. H. Zurek, Phys. Rev. Lett. **99**, 130402 (2007).
[13] H. Saito, Y. Kawaguchi, and M. Ueda, Phys. Rev. A **75**, 013621 (2007).
[14] A. Lamacraft, Phys. Rev. Lett. **98**, 160404 (2007).
[15] G. I. Mias, N. R. Cooper, and S. M. Girvin, Phys. Rev. A **77**, 023616 (2008).
[16] R. W. Cherng *et al.*, Phys. Rev. Lett. **100**, 180404 (2008).
[17] L. E. Sadler *et al.*, Nature (London) **443**, 312 (2006).
[18] M. Vengalattore *et al.*, Phys. Rev. Lett. **100**, 170403 (2008).
[19] J. D. Sau *et al.*, Phys. Rev. A **80**, 023622 (2009).
[20] R. W. Cherng and E. Demler, Phys. Rev. Lett. **103**, 185301 (2009).
[21] Y. Kawaguchi *et al.*, arXiv:0909.0565 [Phys. Rev. A (to be published)].
[22] C. Klempt *et al.*, Phys. Rev. Lett. **103**, 195302 (2009).
[23] J. Kronjäger *et al.*, Phys. Rev. Lett. **97**, 110404 (2006).
[24] Note that the slight residual axial magnetic field variation in our experiment could possibly influence the patterns observed at the lowest magnetic field $B = 80$ mG.
[25] T.-L. Ho, Phys. Rev. Lett. **81**, 742 (1998).
[26] T. Ohmi and K. Machida, J. Phys. Soc. Jpn. **67**, 1822 (1998).
[27] C. V. Ciobanu, S.-K. Yip, and T.-L. Ho, Phys. Rev. A **61**, 033607 (2000).
[28] For $F = 2$, the crossover resonance between interaction and Zeeman regime occurs at roughly $g_1 n/q = 0.5$ [35]
[29] S. Hofferberth *et al.*, Nature (London) **449**, 324 (2007).
[30] A. Widera *et al.*, Phys. Rev. Lett. **100**, 140401 (2008).
[31] C. Klempt *et al.*, Phys. Rev. Lett. **104**, 195303 (2010).
[32] S. R. Leslie *et al.*, Phys. Rev. A **79**, 043631 (2009).
[33] At the observed growth rates (20.5 s^{-1} and 28.5 s^{-1}, respectively), an initial modulation is amplified by roughly factor of 100 during the phase of linear evolution. Assuming a modulation depth of 50% at the end of this phase implies an initial depth of 0.5%. By comparison, at a linear density of 1700 μm^{-1} the shot noise of atoms contained within one half wavelength is 0.6%–0.7%.
[34] M. Matuszewski, Phys. Rev. Lett. **105**, 020405 (2010).
[35] J. Kronjäger, K. Sengstock, and K. Bongs, New J. Phys. **10**, 045028 (2008).